PHYSICAL REVIEW A VOLUME 40, NUMBER 3 AUGUST 1, 1989

Equilibrium statistical mechanics for kinetic phase transitions

Dana A. Browne
Department of Physics and Astronomy, Louisiana State University, Baton Rouge, Louisiana 70803

Peter Kleban
Baker Laboratory, Cornell University, Ithaca, New York 14853
and Laboratory for Surface Science and Technology and Department of Physics and Astronomy, University of Maine, Orono, Maine 04469*

(Received 5 December 1988)

We consider kinetic models for irreversible processes that exhibit nontrivial steady states and phase transitions between these states. We study the steady states of these nonequilibrium systems using the methods of equilibrium statistical mechanics. To accomplish this, we use two methods for associating an effective Hamiltonian $H_{\rm eff}$ with a given steady state. Varying the kinetic rate parameters changes $H_{\rm eff}$, which can lead to phase transitions. Since $H_{\rm eff}$ is defined indirectly, the transitions may occur via new mechanisms not possible in equilibrium systems. We apply these methods to several one-dimensional lattice models relevant to certain aspects of catalysis. Two of these models exhibit second-order phase transitions, one to a catalytically inactive state, the other to a catalytically active state. The transitions are in different universality classes. We employ a model used in polymer unbinding and wetting transitions to investigate these transitions.

I. INTRODUCTION

The dynamical evolution of a system with many degrees of freedom can be described by a set of kinetic rules. For example, a master equation can be used to study the time evolution of the probability distribution for possible configurations (states) of the system. The rate parameters in the master equation specify the rate of change between configurations connected by a single-step process. Under quite general conditions, namely as long as the kinetic rules conserve probability and also allow the system to go from any given configuration to any other configuration in a finite number of steps, the configuration probability distribution will approach a unique nonzero steady-state value ρ. One can imagine more complicated situations arising in the infinite-volume limit, but we have seen no evidence for this in the models we investigate below.

A system which is not in thermodynamic equilibrium may be described by kinetic rules which do not satisfy detailed balance. For example, a transition between two configurations may be allowed, but not the reverse transition. Consider, for example, the total absence of back rates for certain transitions in some of the models defined below. Such kinetic rules, not satisfying detailed balance, may seem unphysical and therefore irrelevant. However, the net rate (state probability times transitions rate) in a given direction may in fact be very small out of equilibrium if the probability is kept low by the steady state, e.g., by appropriate flow conditions or if the transition rate is small. Then it is a reasonable approximation to neglect the rate altogether.

When detailed balance is not obeyed, the steady-state distribution ρ is not simple to determine. However, under the conditions cited, it will exist, and one can define the corresponding effective Hamiltonian via

$$H_{\rm eff} = -\ln(\rho) , \tag{1}$$

where we have set $k_B T = 1$ for convenience. Thus Eq. (1) assigns an effective energy to each configuration of the system and, conversely, ρ is the equilibrium probability distribution for $H_{\rm eff}$. Note that the normalization of ρ implies a particular choice of the zero of energy in $H_{\rm eff}$.

Now for application to a specific kinetic system, the above equation will only be of practical value if $H_{\rm eff}$ can be calculated. When this is possible, the properties of the steady state(s) may be described using equilibrium statistical mechanics, since the information in $H_{\rm eff}$ will be fully equivalent to that in ρ. Thus one can study the behavior of irreversible, kinetically defined systems by mapping them onto an equivalent effective Hamiltonian for a system in thermal equilibrium.

We emphasize that the effective Hamiltonian is merely a shorthand for describing the steady-state probability distribution ρ. Since its definition follows entirely from nonequilibrium kinetics, it has no particular connection with the actual physical Hamiltonian of the system under consideration. It means that the particular "energy" of a state as defined in Eq. (1) may be quite different from its real energy. For instance, in a laser in steady state, the level of highest energy becomes, due to population inversion, the level of lowest effective energy. As we will see, $H_{\rm eff}$ is nonetheless useful because it allows one to apply the concepts and methods of equilibrium statistical mechanics to kinetically defined steady states.

Since there is no simple general method for determining ρ from the master equation when detailed balance is not satisfied, one must follow a more indirect route. In this work we employ two methods. In the first, the kinet-

ic rules are used in a Monte Carlo simulation of a large system (typically 16 348 or 32 768 sites). The resulting configurations are used to compute various correlation functions. Then the effective Hamiltonian is determined by using a set of correlation identities[1-3] which relate the correlation functions to the coupling constants in H_{eff}. The same technique is employed in the Monte Carlo renormalization-group method.[4]

The second method is a direct evaluation of ρ by repeated application of the evolution operator to an assumed initial value for ρ. This method is limited to small systems (chains of length up to 18 sites are treated below) but has the advantage of providing a complete characterization of the steady state and H_{eff}. We find that it gives more accurate and complete results for the interactions than the Monte Carlo simulations, even though the systems are small. In particular, the correlation method cannot reliably compute long-range interactions from the Monte Carlo data, although it does reproduce the short-range interactions reasonably well even in their presence.

The results of such determinations of H_{eff} may be very interesting in cases where the kinetic rules depend on adjustable parameters such as reactant arrival rates and reaction probabilities. Then the steady-state distribution ρ and H_{eff} will also depend on these parameters. Since the connection between the kinetic rules and H_{eff} is not simple, varying the kinetic rate parameters can change H_{eff} in unusual ways which are not possible for equilibrium systems. In this way nonequilibrium or kinetic phase transitions—changes between kinetically defined steady states ρ with qualitatively different properties—can occur by means of mechanisms not found in equilibrium phase transitions. For example, we will find that some one-dimensional systems with simple short-range kinetic rules can exhibit phase transitions. Our analysis of these models in terms of H_{eff} then allows interpretation of the transitions in terms of equilibrium statistical mechanics.

In this paper the techniques just described are applied to several kinetic models defined on one-dimensional lattices. These particular models are designed to illustrate the points made above in a simple context, and were inspired by recent work on models[5,6] incorporating effects of density fluctuations and spatial correlations on heterogeneous catalysis. They resemble the two-dimensional model of Tang and Bak[7] which is also defined via local kinetic rules. We use our effective Hamiltonian, as well as information from the correlations themselves, to probe the mechanisms underlying the transitions.

The paper is organized as follows. In Sec. II we recall the correlation identities,[2,3] and the technique[4] of obtaining interactions from them. Then the direct method for constructing ρ and thereby H_{eff} is briefly described. In Sec. III we define the five different one-dimensional lattice-gas models to be studied and present the results of our analysis. These models include two that exhibit second-order-kinetic phase transitions. We argue that a good model for these transitions is the "necklace" model, which describes the helix-coil transition in polymers and wetting transitions.[8] This model studies the statistics of strings of "beads" (coiled polymers) separated by vacancies (uncoiled polymers) and we find that certain clusters in our models obey the same statistics as the beads. Exponents are given for the second-order transitions. We also contrast our results for each model with the mean-field treatment[9] of the reaction process. Section IV contains our conclusions. The Appendix discusses several new simplifications of the correlation method for calculating H_{eff} that occur when used with lattice-gas Hamiltonians and gives some details of our Monte Carlo simulations.

II. METHODS FOR CALCULATING H_{eff}

This section outlines the methods employed to calculate H_{eff}. In the correlation method, a set of identities[1-3] that connect correlation functions with the coupling constants of the Hamiltonian for lattice-gas systems are used[4,10] to extract the latter given the former. We emphasize that, for a Hamiltonian with a given set of terms, these equations are exact. It is also important that, again if one knows the specific interactions that appear in the Hamiltonian, all the coupling constants may be recovered if a sufficient number of correlation functions are available.

The detailed derivation of these relations has been published elsewhere[1,2,4] so we will confine ourselves to a recapitulation of the underlying idea. Consider a lattice-gas model in thermal equilibrium. By performing a partial trace over a particular occupation number variable n_i, one may replace it, in any average over the configuration probability distribution, with a function depending on all the other occupation number variables and the coupling constants included in interactions with the ith site. Using this one may derive an arbitrary number of equations linear in correlation functions with coefficients that are functions of the coupling constants. For example, consider a one-dimensional lattice gas with the Hamiltonian

$$H=\sum_i (K_0 n_i + K_1 n_i n_{i+1}) \ . \tag{2}$$

One then finds

$$\langle n_i P\rangle = \langle [A + B(n_{i+1}+n_{i+1}) + C n_{i-1} n_{i+1}] P\rangle \ , \tag{3}$$

where P is any function of occupation number variables except n_i, and

$$\begin{aligned} A &= \frac{1}{1+e^{K_0}} \ , \\ B &= \frac{1}{1+e^{K_1+K_0}} - A \ , \\ C &= \frac{1}{1+e^{K_0+2K_1}} - 2B - A \ . \end{aligned} \tag{4}$$

So by suitably choosing P one may find two independent relations solvable for K_1 and K_0 if the appropriate correlation functions are known. Equation (3) is easily generalized to Hamiltonians with terms of arbitrary type, including longer-range pair interactions and multiparticle

terms. In the models analyzed below, the necessary correlation functions are obtained via Monte Carlo simulation of large systems (chains typically of length 32 768 sites), so that the resulting interactions may be compared with those found for short chains via the direct method. A more detailed discussion of how we used the correlation function method is relegated to the Appendix.

Now we briefly consider the second or "direct" method of evaluating the configuration probability distribution ρ and thereby H_{eff} from the kinetic rules. The master equation is

$$\frac{dP_i}{dt} = \sum_j W_{ji} P_j - \sum_j W_{ij} P_i \ , \tag{5}$$

where $P_i(t)$ is the probability of finding the system in state i at time t and W_{ij} is the rate for a transition from state i to state j. The eigenvalues λ_i of the right-hand side satisfy $0 \leq \lambda_i < 1$. It follows that the operator $W_{ij} + W_{ii}\delta_{ij}$, repeatedly applied to an initial state, projects out the steady state. In the calculations below the blank lattice is the initial state.

For the models studied, the convergence of this procedure may be tested by comparing the results with certain exactly known ratios of ρ values; in particular, the chemical potential (on-site energy) is exactly known in each case. We have been able to treat systems of up to 18 sites. The number of iterations required for good convergence varies with the model and lattice size. Up to 50 000 iterations were used for the cluster transition model (defined below) with 12 sites. ρ was calculated with double precision for some models to test for roundoff errors.

Note that in applying Eq. (1) one will obtain the total effective energy for each state from ρ. In order to extract the coupling constants for the various interactions [e.g., K_0 and K_1 in Eq. (2)] one must subtract the interaction energy of each possible subcluster of particles from the total energy of a given state. We report both total energies and coupling constants below.

III. MODELS AND RESULTS

In this section we define the kinetic models to be studied. These are one-dimensional one-component lattice-gas systems. They are of interest in studying the effects of density fluctuations and spatial correlations on catalytic behavior and also as simple irreversible systems exhibiting phase transitions. Our models are inspired by the more complicated two-component two-dimensional systems introduced by Ziff *et al.*[6] The restriction to one dimension may seem artificial, but we note that CO oxidation on Pd(110) has been reported to proceed one dimensionally in a certain pressure and temperature range.[11]

Consider a chain of N adsorption sites labeled by the index i, with periodic boundary conditions. A configuration of the system is specified by assigning the value 0 (empty) or 1 (occupied) to the occupation number variable n_i at each site i. Thus $n_i = 1$ corresponds to the presence of an atom of type A at the ith site. In describing particular configurations we will use a notation like ($AxAAAx$), where the A denotes an occupied site and the x an empty one.

We now describe five sets of kinetic rules, defining five different models. According to these rules A atoms may adsorb and A_2 molecules desorb from the chain; thus, the overall reaction is $A + A \rightarrow A_2$ and our systems model heterogeneous catalysis under irreversible steady-state flow conditions. Table I tabulates the models. We first specify the rules common to all of them. A atoms impinge on the chain at random at some rate γ per site. The value of γ serves only to define the unit of time and has no effect on the steady-state distribution ρ. If a given site i is empty ($n_i = 0$), and is surrounded by empty sites on either side, adsorption occurs. If the site is already occupied ($n_i = 1$), the atom is reflected from the chain and

TABLE I. Kinetic rules defining the one-dimensional models. The initial states are listed in the leftmost column with the A atom impinging on the middle site. The final states for the various models are listed in the other columns. If there is more than one possible final state the rate is given in parentheses. Model IV (alternating-chain transition) interpolates between model II (short range) at $p=0$ and model III (alternating chain) at $p=1$. Model V (cluster transition) also coincides with model II at $p=0$.

Initial state	Model I	Model II	Model III	Model IV	Model V
xxx	xAx	xAx	xAx	xAx	xAx
xxA	xxA	xxx	xxx	xxx	xAA (p)
					xxx $(1-p)$
Axx	xxx	xxx	xxx	xxx	AAx (p)
					xxx $(1-p)$
AxA	xxA	Axx $(\frac{1}{2})$	AxA	AxA (p)	AAA (p)
		xxA $(\frac{1}{2})$		Axx $\left(\frac{1-p}{2}\right)$	Axx $\left(\frac{1-p}{2}\right)$
				xxA $\left(\frac{1-p}{2}\right)$	xxA $\left(\frac{1-p}{2}\right)$

no change in the configuration occurs. If $n_i=0$ and one or both of the neighboring sites is occupied, then depending on the model, (1) an A_2 molecule may be formed and immediately desorb, (2) adsorption may occur, or (3) the configuration is unchanged. There is no diffusion of adsorbed species along the chain, and no desorption in the absence of A_2 formation. Thus the models describe catalytic processes for which the rate-limiting step is the adsorption of an atom at an active site on the chain and include the effects of density fluctuations and spatial correlations in one dimension.

A. Model I (hard cores)

In model I, desorption of an A_2 molecule from site i occurs if the site to the left of i is occupied, regardless of the occupancy of the site to the right of i. If only the site to the right is occupied, the impinging atom is reflected, and there is no change of configuration. (One can exchange "right" and "left" in these rules without altering the results). Standard methods[12] show that this set of kinetic rules satisfies detailed balance, and indeed describes a one-dimensional lattice gas with nearest-neighbor exclusion, and no further interactions. Thus the steady state has no nearest-neighbor pairs of A atoms.

The direct method, for a chain of 12 sites, gives $\langle n_i \rangle = 0.276\,39\ldots$ and all interactions zero to double precision after 2000 iterations. For the correlation method we used Monte Carlo simulation on a lattice of 32 768 sites, and a total of 60 000 Monte Carlo steps (MCS). This gave $\langle n_i \rangle = 0.2765 \pm 0.0016$. Using the correlation method we calculated all interactions of a given site with clusters of up to m adjacent sites, increasing m from 1 to 7. For $m \leq 4$ all coupling constants were no larger than 0.005 in magnitude. For larger m values the largest coupling increased; e.g., for $m=7$ the interaction energy of ($AxxAxAxA$) (the worst case) is equal to -0.039, although the four other symmetry equivalent states have been much smaller coupling constants (the average of the four values is -0.0101). This increasing lack of precision with m is apparently due to the increasing number of terms that must be subtracted to calculate the couplings as m grows, and is also observed in the other models investigated. For a model with unknown interactions this poses the problem of determining whether the effect is due to numerical problems, as here, or the presence of long-range interactions. One way to test for long-range interactions under these conditions is by examining the pair-correlation function. For the hard-core model it decays very quickly with distance to its asymptotic value, as shown in Fig. 1.

Solving the rate equations in mean-field approximation[9] for the concentration of adsorbed A atoms gave $\langle n \rangle = 0.382$ and 0.2764 in single-site and pair approximation, respectively. Since the longest-range interaction is nearest neighbor in this case, retaining nearest-neighbor correlation effects via the pair approximation gives quite accurate results.

The reversibility of this model might seem to contradict the overall reaction $A + A \rightarrow A_2$. However, the true reversibility (or irreversibility of the other models considered) in fact arises by consideration of the states of the chain only; one could regard the removal of two A atoms as part of an $A \rightarrow A$ reaction which is reversible when the chain kinetics are reversible.

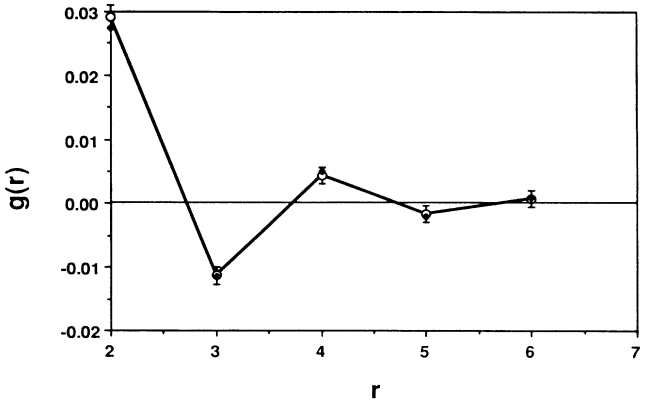

FIG. 1. Pair correlation function $g(r)=\langle n_i n_{i+r} \rangle - \langle n \rangle^2$ for model I (hard core), open circles; and model II (short range), diamonds. Errors are shown for model I, those for model II are similar.

B. Model II ("short range")

Here, A_2 formation and subsequent desorption occurs whenever either neighboring site is occupied. If both are occupied, one of the neighboring A atoms is chosen at random and the other remains adsorbed. These are natural physical assumptions for a model of catalysis of this type. Since, in any allowed configuration under these rules, nearest-neighbor AA pairs are still not permitted, H_{eff} again has a nearest-neighbor exclusion (hard core). However, the change of rules from model I induces additional interactions. Table II presents results of the correlation and direct methods. One sees again that the correlation method is most accurate for clusters that are not too large; this is not surprising since the kinetics do not differ greatly from model I. Table II includes the largest terms, which are all of short range, hence the model's appellation. It should be realized, however, that the energy of a given state (in this or any other model) may also include contributions from a large number of small interactions. For instance, if one keeps only the four largest coupling constants for this model, the energy of the state with six particles (for a chain of length $N=12$) is 2.2285 above the ground state, compared to 2.2098 for the exact value. This occurs even though all of the interactions not included have magnitudes less than 0.0057, and most are at least an order of magnitude smaller than this. The pair correlation is again of short range, as shown in Fig. 1. The mean-field treatment gives $\langle n \rangle = 0.29$ and 0.2265 in site and pair approximation, respectively. Since the large interactions are not of long range these values are accurate, though less so that for the hard-core model. The $\langle n \rangle$ values obtained from the short-chain (0.232 756 for $N=12$) and Monte Carlo methods ($0.232\,8 \pm 0.002\,0$) agree, as shown in Fig. 4 (discussed later).

TABLE II. Coupling constants for the short-range model (II). The correlation method results, from left to right, refer to clusters with $m=4,5,6,7$ (see Appendix).

Cluster	Direct	$m=4$	$m=5$	$m=6$	$m=7$
A	ln2	0.687	0.687	0.684	0.672±0.02
AxA	−0.300	−0.295	−0.291	−0.292	−0.231±0.05
$AxxA$	0.001	0.011	0.013	0.015	0.021±0.002
$AxxxA$	0.014	0.016	0.015	0.017	0.025±0.02
$AxAxA$	−0.036	−0.039	−0.042	−0.038	−0.046±0.02

Note that the short-range model contains some transition pathways that do not satisfy detailed balance. Consider a system of six sites and the configurations ($AxAxAx$) and ($xxxxxx$). There are two ways to get from one to the other, depending on the order in which A atoms are removed, and the products of reaction rates around the resulting loop of configurations differ according to the direction taken.[13]

C. Model III (alternating-chain model)

This is the same as the short-range model, except that when both sites adjacent to site i are occupied, the impinging A atom is reflected. This kind of effect might occur on a real catalyst if second-neighbor AA forces are sufficiently attractive to prevent association of A atoms. It results in configurations favoring long *alternating chains* of ($AxAxAx\ldots$). There are many configurations leading to a given one with such chains, via adsorption of an A atom, but the chain can only be removed by desorption from the ends, so in this sense detailed balance is more strongly violated than in the short-range model. The absence of AA pairs again implies a hard core, but the additional interactions required to sustain the alternating chains are considerably stronger and more long ranged than for the short-range model, as may be seen on comparing Tables II and III. For this reason the mean-field treatment is considerably less accurate, giving $\langle n \rangle = 0.33$ and 0.25 in site and pair approximation, respectively, as opposed to 0.43 from the Monte Carlo calculation (see below).

TABLE III. Coupling constants for the alternating-chain model (III). The direct method results are for chain length $N=15$; the correlation method is, from the left for $m=6$ and 7. All direct terms with coupling larger than 0.1 in magnitude, and for no more than 8 sites, are included; however, the correlation method shows some additional terms with couplings >0.1. The difference between the two methods is greater than for the short-range model shown in Table II and is probably due to the longer range of the interactions.

Cluster	Direct ($N=15$)	$m=6$	$m=7$
A	ln2	0.708	0.768
AxA	−0.906	−0.861±0.02	−0.829±0.03
$AxxxA$	0.256	0.200±0.03	0.090±0.03
$AxxAxA$	−0.523	-0.458 ± 0.04	$-0.488^{+0.02}_{-0.13}$
$AxxAxA$	0.103	0.131±0.08	0.071±0.10
$AxAxAxA$	−0.312	−0.388±0.22	−0.352±0.24

If the total number of sites N is even, this model (recall the periodic boundary conditions) has a catalytically inactive (or poisoned) state[6] in which every other site is occupied. There is no way to leave this configuration, and therefore the conditions for the existence of a unique steady state are, strictly speaking, not satisfied. As a result the direct method of calculating ρ does not converge; the catalytically inactive state becomes more probable with the number of iterations and the concentration $\langle n \rangle$ approaches 0.5. On the other hand, when N is odd this configuration is not possible, and ρ gives rise to an H_{eff} with a few short-range interactions and some longer-range ones involving alternating chains (see Table III).

The states with single alternating chains have the lowest total energy, and the variation of their energy with chain length is shown in Fig. 2(a). We suspect that these states (or similar ones) are important for the phase transitions discussed below; similar behavior will be seen in other models as well. It is perhaps significant that their total energy is in general not given by the sum of the largest interaction terms, but rather involves important contributions from many small couplings.

The Monte Carlo simulations, performed with $N=32\,768$, indicate that the steady state is not trivial in the large N limit. They give $\langle n \rangle = 0.4302\pm0.0036$. The presence of long alternating chains in this model tends to slow the convergence of the Monte Carlo simulations, since all the changes occur in the relatively rare regions between chains. However, we believe our result for $\langle n \rangle$ to be accurate. Indeed, simulations starting from an initially blank state, discarding the first 20 000 MCS/site, and sampling every 500 MCS/site for the next 60 000 MCS/site gave $\langle n \rangle = 0.430\pm0.007$. Starting from the final configuration of this first run and making a second run for 50 000 MCS and sampling every 100 MCS/site gave $\langle n \rangle = 0.4302\pm0.0036$.

It might be thought that a typical configuration for this model consists mainly of long alternating chains separated by short regions of simple "defects," or domain walls. However, examination of the Monte Carlo results shows that there is a wide variety of chain lengths and defect types and lengths present. Thus the dynamics does not appear to be simple. The behavior of the pair correlation function (Fig. 3) is one indication of this. It is very long ranged and reproduced well within the error by the form

$$g(r)=(-1)^r[0.0907\exp(-r/12.09) + 0.1129\exp(-r/68.44)]\ , \qquad (6a)$$

over the range $10<r<100$. However, at larger r values $g(r)$ appears to obey a power-law form,

$$g(r)=\frac{\text{const}(-1)^r}{r^{-1+\eta}} \tag{6b}$$

with the rather large exponent $-1+\eta\approx 2.2$ as shown in Fig. 3. This suggests that the alternating-chain model is at critcality, consistent with our results for the chain transition model discussed below.

However, since the kinetic rules strongly favor the passivated state, the presence of two well-separated length scales in the correlation function could indicate that the alternating-chain model steady state is a coexisting phase in the thermodynamic limit. We now examine this possibility, and show that the available evidence rules it out. For a coexisting phase one has

$$\rho=\lambda\rho_e+(1-\lambda)\rho_0\ , \tag{7}$$

where ρ_e and ρ_0 are two distinct distributions, and $0<\lambda<1$. We first assume that ρ_e and ρ_0 are the limiting

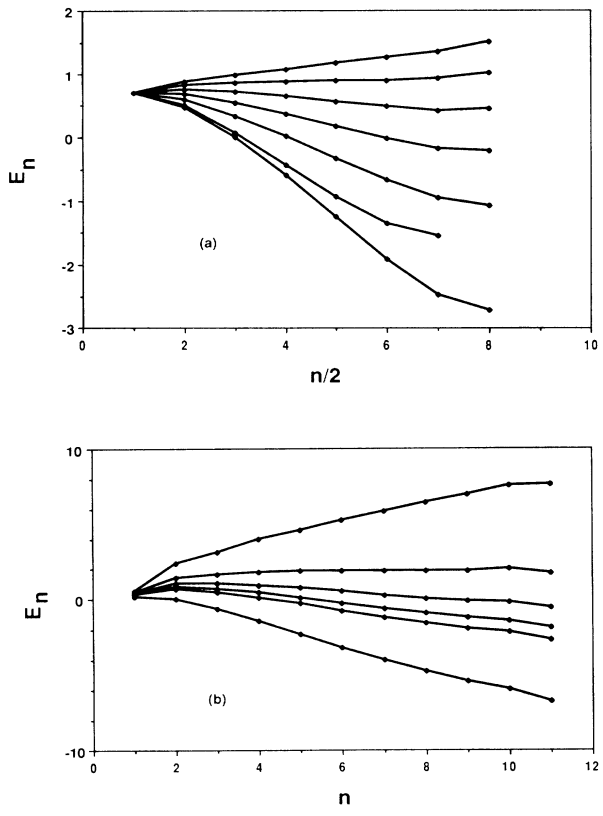

FIG. 2. (a) Total energies E_n of states with a single cluster of n contiguous empty sites as a function of n for the chain transition model. In order from above, the curves show $p=0.5,0.6,0.7,0.8,0.9$ for $N=18$, then $p=0.99$ for $N=16$, and finally the alternating-chain model for $N=17$. (b) Total energies E_n of states with single clusters of n contiguous vacant sites vs n for the cluster-transition model, from chains of length $N=12$. Successive curves show $p=0.1,0.2,0.25,0.28,0.3,0.4$ in order from above.

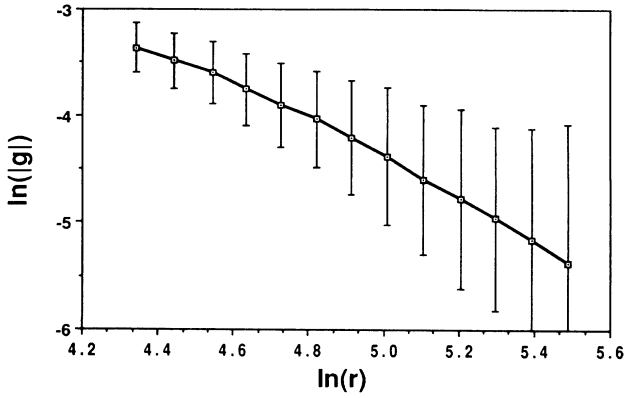

FIG. 3. Magnitude of the pair-correlation function $|g(r)|$ for the alternating-chain model. Note that $g(r)$ is negative at all odd values of r.

distributions for even and odd chains as $N\to\infty$, respectively. Then $\langle n\rangle$ will be an average of even and odd values, $\langle n\rangle=\lambda\langle n\rangle_e+(1-\lambda)\langle n\rangle_o$. Since $\langle n\rangle_e=0.5$, and assuming $\lambda=0.5$, the Monte Carlo result implies $\langle n\rangle_o=0.3604\pm0.0072$ for the limit of odd N values. This is not inconsistent with our short-chain results, which give $\langle n\rangle=0.326$, 0.336, and 0.344 for $N=13$, 15, and 17, respectively. Larger λ values reduce the size of $\langle n\rangle_o$. However, since the correlation function $\langle n_i n_{i+r}\rangle$ for N even is $0.25+0.25(-1)^r$, such a phase would also show a term with long-range order, $0.25\lambda(-1)^r$ as $r\to\infty$. This we definitely do not observe. Within the error we see a small oscillation in the correlation function at large r; if this is attributed to coexistence, it would indicate that λ is 0.002 at most. (For this λ value $\langle n\rangle_o=0.4301$.) We have also checked for long range order by computing the ferromagnetic susceptibility per site

$$\chi_0/N=\left\langle\left[(1/N)\sum_i n_i\right]^2\right\rangle-\langle n\rangle^2$$

via Monte Carlo. This is a useful quantity since χ_0 will be constant for large N unless there is long-range order, in which case it becomes proportional to N. We find $\chi_0/N=0.0\pm10^{-5}$. The staggered susceptibility is also much less than N, as we discuss below.

A second possibility is coexistence between two phases without long-range order. To test for this, first consider the large r limit of $\langle n_i n_{i+r}\rangle$. In a distribution described by Eq. (7), it is given by

$$\langle n_i n_{i+r}\rangle=\lambda(\langle n\rangle_e)^2+(1-\lambda)(\langle n\rangle_o)^2\ .$$

The Monte Carlo results show that this result is different from $\langle n\rangle^2$ by at most 0.005. Assuming that $\langle n\rangle$ for one of the coexisting phases is close to 0.5 then implies that λ may be as large as 0.5 so this kind of coexistence is so far not ruled out. However, there is another more stringent test involving the quantity χ/N mentioned above. For this kind of coexistence it satisfies $\chi/N=\lambda/(1-\lambda)(\langle n\rangle-\langle n\rangle_o)^2$. Now recall χ/N is zero to within

10^{-5} for the alternating chain model. Thus if $\langle n \rangle_o = 0.5$, λ is within 1.8×10^{-3} of 1; conversely if $\lambda = 0.5$, the difference between $\langle n \rangle$ and $\langle n \rangle_o$ is less than 3×10^{-3}. Hence this second type of coexistence does not appear to be present either.

D. Model IV (chain transition model)

This case interpolates between the two previous models by means of an adjustable parameter p, such that $p=0$ is the short-range model and $p=1$ is the alternating-chain model, as shown in Table I. Thus the steady-state distribution ρ and H_{eff} become functions of p. The system exhibits a phase transition at $p=1$.

This model exhibits significant odd-even and finite-size effects. We first describe the behavior of short (up to 18 site) chains. When the number of sites N is odd, the alternating chain model does not poison, and the concentration $\langle n \rangle$ smoothly approaches a limiting value, as illustrated in Fig. 4(a). For N even, $\langle n \rangle$ follows the odd-site curve closely until $p \approx 0.9$, after which it increases rapidly to 0.5. This increase occurs over a range of p values which shrinks as the number of sites grows. For long chains ($N=32$, 768) the Monte Carlo results [Fig. 4(a)] fit neatly between the odd and even short-chain curves, but smoothly approach $\langle n \rangle = 0.4302 \pm 0.0036$ as $p \to 1$, as shown in Fig. 4(b). Thus this model displays a second-order phase transition. The coverage varies near $p=1$ as $(0.4302 - \langle n \rangle) \propto (1-p)^{\beta}$, where $\beta = 0.30 \pm 0.02$. The staggered susceptibility, given by $\chi = \sum_r (-1)^r g(r)$, varies near the transition as $(1-p)^{-\gamma}$. We find from Fig. 5 that $\gamma = 0.40 \pm 0.05$. For the alternating-chain model discussed earlier we find $\chi = 78$; finite-size scaling implies this should be proportional to $N^{\gamma/\nu}$. We therefore estimate $\nu \simeq 1.0$. It is interesting that the value of η given below [Eq. 6(b)] does not satisfy the scaling relation $\gamma = \nu(2-\eta)$.

We gain understanding of this model by considering H_{eff} as a function of p. As p is increased, the interactions derived from the direct solution of a short chain interpolate smoothly between the short-range- and alternating-chain-model results (Tables II and III). Thus the predominant short-range interactions of the short-range model change gradually. In addition, attractive interaction terms where all the atoms are in long alternating chains ($AxAxAx\ldots$) become significant at about $p=0.9$ and increase with p as the model approaches the alternating-chain limit. For chains with an even number of sites, the total energy and coupling constant of the longest alternating-chain configuration (the catalytically inactive state) becomes arbitrarily large and negative as p approaches 1. In fact, the energy difference between this state and the alternating one with one less particle is exactly $\ln(1-p)$. Aside from the alternating chain states, as p approaches 1 all other configurations lie in a band whose energy width stays approximately constant (although increasing slightly near $p=1$) at each N value. The width also increases somewhat with N. For N odd similar behavior occurs except that there is no poisoned state.

These remarks suggest that the states consisting of a

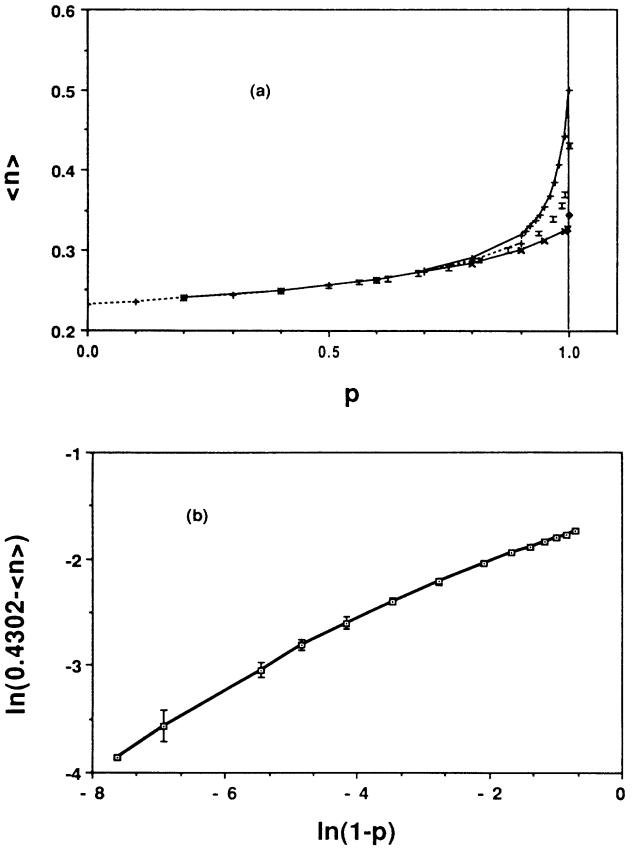

FIG. 4. (a) Concentration $\langle n \rangle$ vs p for the chain-transition model. Note that $p=0$ is the short-range model and $p=1$ is the alternating-chain model. Short-chain results are shown with crosses, center dashed line ($N=18$); crosses, upper line ($N=12$); and $\times$'s on lower line ($N=13$). The triangle at $p=1$ is the value for $N=17$. Monte Carlo results include error bars. (b) $\langle n \rangle$ vs p near the phase transition.

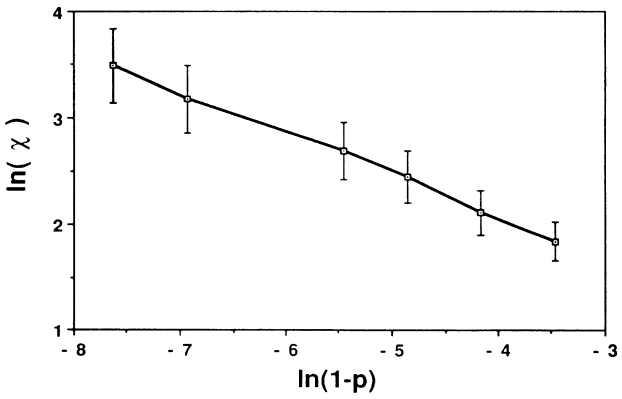

FIG. 5. Ferromagnetic susceptibility per site χ_0/N vs p for the chain-transition model near the transition.

single alternating ($AxAxAx\ldots$) chain of $n/2$ pairs of occupied-unoccupied sites are important in the transition. For short chains the total energy (with respect to the empty state energy) of these clusters is given approximately by the form [see Figs. 4(a)]

$$E_n = A + Bn + b(n) , \tag{8}$$

where $b(n)$, with $b(1)=0$ and $b/n \to 0$ as $n \to \infty$, represents a correction to linearity which is small for large clusters but essential to the phase-transition behavior, as we will see. Note that if we were to write H_{eff} in terms of the interactions between the occupied sites, as in Eq. (2), E_n will involve contributions from many kinds of terms, since it is the *total* energy of this configuration. Equation (8) does not hold for the states of largest n when N is even, since they are influenced by the poisoned state of the alternating-chain model with even N, as discussed below. Also, $E_1 = \ln 2$, independent of p and N. More importantly, at a given p value, there seem to be at most only very small finite-size effects, so that B is independent of N. For small p, B is positive, but it decreases (apparently smoothly) with p, going through zero at $p \approx 0.6$, so that it is defintely negative at the phase transition. Note that this negative value implies the presence of many long alternating chains with a concentration $\langle n \rangle$ close to 0.5. These states may then be responsible for the long correlation length in the alternating-chain model. Some interesting further implications of Eq. (8) are considered later.

Finally, we should note that the mean-field treatment of this model, in site or pair approximation, does not show a phase transition. The concentration simply changes smoothly from the short-range to alternating-chain model value as p goes from 0 to 1.

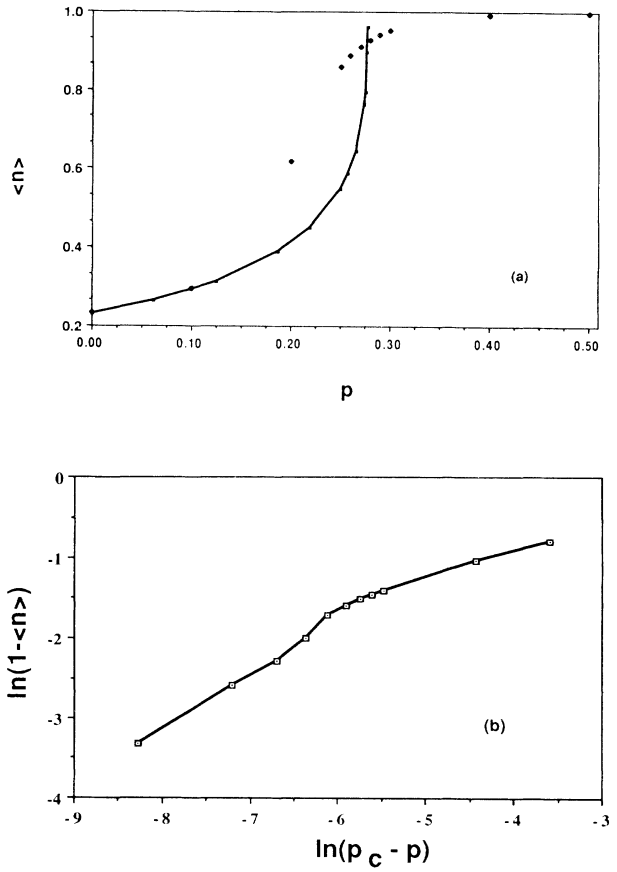

FIG. 6. (a) Concentration $\langle n \rangle$ vs p for the cluster-transition model. Squares are Monte Carlo data. Diamonds are $N=12$ short-chain results. (b) $\langle n \rangle$ vs p near the transition.

E. Model V (cluster transition)

Our final model differs from all the previous cases in that an A atom impinging next to an adsorbed A atom will either adsorb, with probability p, or associate and thereby remove the previously adsorbed atom, with probability $1-p$. If both neighboring sites are occupied, association occurs randomly to either side with probability $(1-p)/2$, as illustrated in Table I. Thus this model has no hard-core repulsion between nearest neighbors for nonzero p.

The parameter p plays a central role in determining the nature of the steady state, and in fact this model exhibits a phase transition as it is varied. For long chains with $p > p_c = 0.2776 \pm 0.0002$ the enhanced possibility of adsorption is sufficient to drive the system to a poisoned state where all sites are occupied and the catalytic activity ceases. As p is reduced below p_c, the concentration of adsorbed A atoms gradually decreases, as shown in Fig. 6(a). Within the accuracy of our data the slope is infinite at p_c, indicating that the phase transition is second order.

Analysis of the $\langle n \rangle$ versus p and pair-correlation function gives critical exponent values. Using the relations $\langle n \rangle \propto (p_c - p)^{\beta}$ and $g(r) \propto \exp(-r/\xi)/r^{-1+\eta}$ with $\xi \propto (p_c - p)^{-\nu}$ for p near p_c, we find $\beta = 0.70 \pm 0.05$, $\eta = 1.30 \pm 0.03$, and $\nu = 1.3 \pm 0.2$, so this model is in a different universality class from the alternating-chain transition.

Since there is no hard core, the number of states increases more rapidly with chain length N than in the previous cases. As a result we were only able to use the direct method for $N \leq 12$. The $\langle n \rangle$ versus p values obtained this way therefore show significant finite-size effects [see Fig. 6(a)]. Deviations from the long-chain Monte Carlo results set in at $p - p_c \simeq 0.2$. For $p = 0.0625$ the correlation length, determined from the long chain, is $\xi = 8 \simeq N$, consistent with the theory of finite-size effects at second-order transitions. With the kinetic rules defined in Table I short chains evolve to the poisoned (completely filled) state for any $p > 0$. To avoid this, we supplemented the rates given by a small desorption probability ϵ for $AAA \to AxA$ and $1-\epsilon$ for $AAA \to AAA$ with ϵ taken proportional to p [$\epsilon/p = 0.001$ for the results shown in Fig. 6(a)]. Making this ratio fives times larger changed the coverage at $p = 0.28$ from 0.923 to 0.776; all the interaction energies remained the same to two figures except for the entirely filled state (for which the coupling changed from -1.83 to -0.482) and the state with one empty site (from -0.14 to -0.12). A ratio ϵ of 0.01 led

to larger changes. Results for $p<0.28$ were much less sensitive to the magnitude of ϵ. Note that the value of this ratio fixes the energy difference between the filled state and the state with one empty site so we have not considered them in the analysis below.

Insight into the mechanism of the phase transition can be gained by examining the short-chain interaction energy results. Note that this model coincides with the "short-range" model at $p=0$. The on-site energy (chemical potential) is $\ln[2(1-p)]$, and thus changes smoothly with p in the region of the transition. The second-neighbor-pair term, equal to -0.260 at $p=0$ becomes less attractive as p increases, passing through zero above $p=0.4$. For a given number of atoms, all terms are small except for the multiparticle interactions of a single cluster of contiguous A atoms. For example, at $p=0.28$ the terms involving four noncontiguous particles are all a factor of 5 or more smaller than the cluster term. Since, unless there are infinite interactions, a phase transition in one dimension necessarily involves long-range forces,[14] these terms are the prime candidates. This, as for the chain-transition model, implies that the corresponding states are of interest. Figure 2(b) shows their energy versus cluster size for various p values near the transition. The behavior of Eq. (8) is found again, suggesting a connection between the two models.

In mean field theory, this model shows a second order phase transition to the $\langle n \rangle = 1$ state. This occurs at $p_c=0.5(0.410)$ in site (pair) approximation. The large error in p_c is another indication that long range forces are important in the transition. The exponent $\beta=0.5$ in site approximation and 1.0 in pair approximation.

F. Necklace mechanism for models IV and V

Next we probe the nature of the phase transition in the cluster transition and chain transition models. We assume that Eq. (8) is the correct form for the energy of the cluster states for large n and that interactions between clusters are unimportant (or included in an effective value of the correction term $b(n)$). Then the model is described by the necklace or bead statistics useful in the theory of the helix-coil transition in polymers and wetting in two dimensions.[8] The interpretation is a bit different here—in particular we have a true one-dimensional model—but the mathematical mechanism is the same. Let $Q(N)$ denote the partition function for a chain of length N including all possible numbers and lengths of clusters, or beads. Then the generating function (isobaric partition function) defined by

$$\mathcal{Q}(z)=\sum_{N=1}^{\infty} Q(N)z^N \tag{9}$$

is given by

$$\mathcal{Q}(z)=\frac{U(z)V(z)}{1-U(z)V(z)}\ , \tag{10}$$

where $U(z)=z/(1-z)$ and

$$V(z)=\sum_{j=1}^{\infty} z^j \exp(-E_j)\ .$$

The precise form of $\mathcal{Q}$ depends on the boundary conditions, but this is unimportant for our purposes. Applying Cauchy's theorem to Eq. (9) and letting $N\to\infty$ shows that the singularity z_0 of $\mathcal{Q}$ closest to the origin determines the free energy per site via $f=\ln z_0$. Now suppose the last term in Eq. (8) has the simple form $b(n)=b\ln n$. Then for $b>1$, a phase transition occurs when the singularity z_0 closest to the origin changes its nature, from the solution of $UV=1$, arising from the denominator of Eq. (10), to $z_0=e^B$, the singularity of $V(z)$. This occurs when B becomes sufficiently negative. For $1<b<2$ the transition is second order. The transition occurs when

$$\zeta(b)=e^A(e^{-B}-1)\ , \tag{11}$$

where $\zeta(x)$ is the Riemann ζ function. Note that a transition at $B<0$ is exactly what we observe for these models. As it is approached, the average number of sites in clusters goes continuously to its saturated value with critical exponents

$$\begin{aligned}\beta&=(2-b)/(b-1)\ ,\\ \nu&=1/(b-1)\ .\end{aligned} \tag{12}$$

We first consider this mechanism for the cluster-transition model. The values for β and ν for this model reported above imply $b=1.59\pm0.02$ and $b\approx1.79\pm0.12$, respectively. On the other hand, Eq. (11) gives $b=1.71\pm0.01$ if we substitute values for $A+B$ and $B+b\ln n$ from values for E_1 and $E_{n+1}-E_n$ [see Fig. 2(b)] and determine b self-consistently from Eq. (8). The exponent γ for the susceptibility χ_0 satisfies $\beta+\gamma=1$ in this model. Our data for χ_0 is rather noisy (Fig. 7) but it indicates a divergence as $p\to1$ with an exponent $\gamma=0.6\pm0.15$ which is consistent with this relation. Note that again the relation $\gamma=\nu(2-\eta)$ does not hold. Our analysis assumes that A and B in Eq. (8) are smooth functions of p near the transition. The good agreement with the predictions of the *necklace* model is very surprising and strongly suggests that is the operative mechanism here. A derivation directly from the kinetic rules for the cluster-transition model would be very interesting.

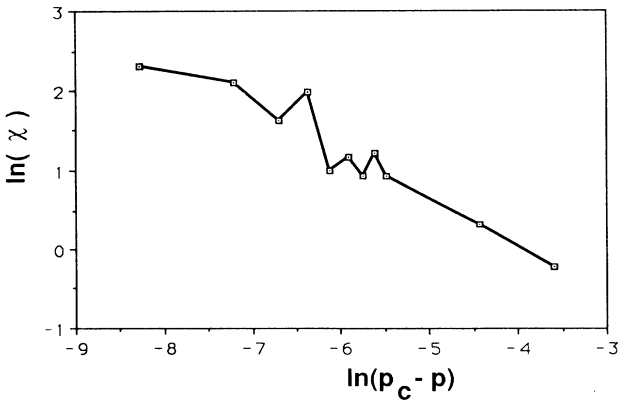

FIG. 7. Ferromagnetic susceptibility per site χ_0/N vs p for the cluster-transition model near the transition.

The chain-transition model also has cluster energies that appear to satisfy Eq. (8). However, to describe this transition with *necklace* statistics requires a more complicated model. First, a necklace transition of the type discussed above is to a catalytically inactive state, whereas the chain transition is to the alternating-chain model which is definitely not poisoned. This could be a result of interactions between the beads. Indeed, the Monte Carlo configurations exhibit a different probability for even- and odd-length interbead chain segments, which is not included in the simple necklace model. A fit to Eq. (11) with $b(n)=b\ln(n)$ gives $b=1.33$, which results in exponents that are very far from the observed values given above; for example, $\beta=2.03$. Of course, this might be due to the form of $b(n)$ being different at small n from its asymptotic form, which would affect Eq. (11) but not the exponents. However, the exponents for this model do not satisfy the necklace model relation $\beta+\gamma=1$. This may also be due to interactions.

IV. CONCLUSIONS AND FUTURE WORK

We have examined a series of one-dimensional lattice-gas models relevant to heterogeneous catalysis. They are defined by a set of kinetic rules which do not obey detailed balance. Phase transitions between the various steady states are seen as the kinetic parameters are varied. We have connected these features to equilibrium statistical mechanics via effective Hamiltonians. We have used two different methods here to calculate the effective Hamiltonians and found substantial agreement. The two models exhibiting second-order phase transitions can be described via the necklace mechanism originally introduced to discuss polymer unbinding and wetting transitions. In the chain-transition model it appears that the necklace model needs to include interbead interactions in order to correctly describe the transition.

In future work we plan to use the correlation function method to analyze the interesting but more involved models of Ref. 6 similarly. The required extension of our method is completely straightforward, the only complication being that for a given range of interaction more terms may appear in H_{eff} and correspondingly more correlation functions are required to solve for them. It is worth noting, in this context, that the good agreement obtained from the mean-field treatment of Ref. 9 for the CO oxidation model of Ref. 6 indicates the absence of long-range forces in H_{eff}, at least in the vicinity of the first-order transition; hence the correlation method is expected to give accurate results. In a preliminary study, we have performed Monte Carlo simulations of this model in one dimension and find that the region of nonvanishing CO_2 formation is very small at best, consistent with the results of Ref. 5.

ACKNOWLEDGMENTS

We would like to acknowledge stimulating and useful conversations with R. H. Swendsen, B. Widom, M. E. Fisher, K. A. Dawson, S. R. McKay, M. Gelfand, R. Durrett, and A. N. Becker. Thanks are due to J. Barry for bringing Ref. 1 to our attention. D. A. Browne was supported in part by National Science Foundation under Grant No. DMR-84-17555 while at Cornell University, where much of this work was done; from the Council on Research at Louisiana State University, and by the Laboratory for Surface Science and Technology at the University of Maine. P. Kleban acknowledges the hospitality of M. E. Fisher and Baker Laboratory, Cornell University.

APPENDIX

In this appendix we will discuss at some length the details of the Monte Carlo simulations and their analysis via the correlation-function method.[1-4] The reason for this detail is that this method is usually applied to spin systems, not lattice-gas models, and we want to point out that a considerable amount of simplification, and some numerical stability, appears when using the lattice-gas versions of the equations.

The Monte Carlo simulations were quite straightforward. For the "hard-core," "short-range" and "alternating-chain" models, the simulations were performed on a chain of length 32 768 while the "chain-transition" and "cluster-transition" models, the chains were of length 16 384. In each case periodic boundary conditions were employed. The latter models were also studied for chains of length 128, 1024, and 4096 to examine finite-size effects near the transition. For most of the work we started with an initially blank chain. We also examined the effect of using a state from one model as the initial state for another of the models, but the rate of relaxation and the final steady state reached were not noticeably different. It appears that the rapid filling in of the blank lattice over the first 30 MCS/site gives a good starting point. However, we erred on the side of conservatism and thermalized each model for 20 000 MCS/site. This was more than sufficient for the hard-core, short-range, and cluster-transition models, which have no obvious slow relaxation modes, while the alterating-chain model relaxed more slowly due to the long strings of $(AxAxAx\ldots)$ that occur. After thermalizing, the data were typically sampled every 500 MCS/site over an additional 60 000 MCS. Then a second run of 60 000 MCS starting from the final configuration of the first run was made and sampled more frequently (100 MCS/site). By comparing the second run with the first, we could look for longer-term drifts in the coverage and the pair correlations; only the alternating-chain and chain-transition model near $p=1$ showed any evidence of drift, and it was small. One reason for all this work was that the net production rate of A_2 was essentially constant (to at least four significant digits) over the *entire* run, and so it provided a poor measure of when the system had reached the steady state, contrary to our initial expectations. It appears that there are large-scale rearrangements in the particle distribution that occur en route to be the steady state that do not significantly affect the production rate of A_2.

In the correlation-function method analysis,[2,3] it is necessary to devise a method that produced reasonably

good values for the cluster energies despite the rather small number of configurations (<600) used in computing the correlation functions. The method we arrived at is particularly simple in the lattice-gas language as opposed to the more common spin description.

We will demonstrate the method with the simple model mentioned in Sec. II, namely the nearest-neighbor lattice-gas model, since the extension to longer-ranged and cluster interactions is just a matter of detail. The terms in the Hamiltonian that depend on the state of the ith site are given by

$$H_i=[K_0+K_1(n_{i-1}+n_{i+1})]n_i \ . \tag{A1}$$

Defining $f(x)=1/[1+\exp(x)]$, we have

$$\begin{aligned}\langle n_iP\rangle=&f(K_0)\langle P\rangle+[f(K_1)-f(K_0)]\langle(n_{i+1}+n_{i-1})P\rangle\\&+[f(2K_1+K_0)-2f(K_1+K_0)\\&+f(K_0)]\langle n_{i-1}n_{i+1}P\rangle \ .\end{aligned} \tag{A2}$$

To get a closed set of equation for K_1 and K_0, three obvious choices for P are $P=1$, $P=n_{i+1}+n_{i-1}$, and $P=n_{i+1}n_{i-1}$. The resulting equations can then be solved for the combinations of differences of f's. However, the statistical uncertainties in the various correlation functions combined with the large number of subtractions of terms with comparable magnitude in Eq. (A2) cause both the total energy of a cluster and the individual coupling constants to have large errors associated with them. It turns out that a smaller error in the cluster energy arises if Eq. (A2) is rewritten as

$$\begin{aligned}\langle n_iP\rangle=&f(K_0)\langle(1-n_{i-1})(1-n_{i+1})P\rangle\\&+f(K_1)\langle[n_{i+1}(1-n_{i-1})+n_{i-1}(1-n_{i+1})]P\rangle\\&+f(2K_1+K_0)\langle n_{i-1}n_{i+1}P\rangle \ ,\end{aligned} \tag{A3}$$

which immediately suggests the set

$$P=(1-n_{i-1})(1-n_{i+1}) \ ,$$

$$P=[n_{i+1}(1-n_{i-1})+n_{i-1}(1-n_{i+1})] \ ,$$

and

$$P=n_{i-1}n_{i+1} \ .$$

These three choices are very useful since they are "orthogonal" in the sense that only one of them can occur in a given configuration at a time. As a result, Eq. (A3) can be trivially solved to yield

$$\begin{aligned}\exp(-K_0)&=\frac{\langle n_i[(1-n_{i-1})(1-n_{i+1})]\rangle}{\langle[1-n_i][(1-n_{i-1})(1-n_{i+1})]\rangle} \ ,\\ \exp[-(K_0+K_1)]&=\frac{\langle n_i[n_{i+1}(1-n_{i-1})+n_{i-1}(1-n_{i+1})]\rangle}{\langle(1-n_i)[n_{i+1}(1-n_{i-1})+n_{i-1}(1-n_{i+1})]\rangle} \ ,\\ \exp[-(K_0+2K_1)]&=\frac{\langle n_i(n_{i+1}n_{i-1})\rangle}{\langle(1-n_i)(n_{i+1}n_{i-1})\rangle} \ .\end{aligned} \tag{A4}$$

We wish to stress that these relations are *exact* for the given model and will change if the couplings are of longer range or include larger clusters of sites. These relations show simply that the free energy of a given cluster (xAx), (AAx), (xAA), or (AAA), which is the argument of the exponent in each of the above equations (A4), is simply related to the ratio of the probability of finding such a cluster to the probability of finding a cluster which differs only in having the site i empty. That is, it is the free-energy gain in completing the cluster. Since larger clusters have many choices for the final site that completes it, one gets several estimates for the cluster energy and hence can reduce the statistical error.

In applying this method to our Monte Carlo data, we started by assuming the model of (A1) which includes all interactions with neighbors up to one lattice site away and then found the couplings. We would repeat this process, increasing the maximum range of the couplings by one each time. For example, the first iteration of this process would add to H_i the coupling terms

$$\begin{aligned}&K_2n_i(n_{i+2}+n_{i-2})\\&\quad+K_3n_i(n_{i+1}n_{i-1}+n_{i+1}n_{i+2}+n_{i-1}n_{i+1}) \ .\end{aligned}$$

This process was stopped when the new couplings that appeared at each step were small and the short-ranged couplings settled down to well-defined values, or the number of terms became so large that the noise in each term started to exceed the size of the long-range couplings. For the Monte Carlo data, this typically occurred by the 7th iteration, i.e., when all couplings up to seven sites away were included. Of course, for the exact solution of the short chains this process was only limited by the size of the chain.

The principal disadvantage of the correlation-function method when applied to the Monte Carlo simulations that we encountered was in the evaluation of the short-range interactions, say the chemical potential or nearest-neighbor coupling, in a system with long-range interactions that is nearly poisoned. In that case it is difficult to get enough configurations to give reliable estimates for the two probabilities in Eq. (A4). For example, in a system with a large attractive interaction for 5 adjacent atoms as well as some shorter-ranged couplings, evaluation of the chemical potential requires us to determine the ratio of the probability of observing a configuration ($xxxxxAxxxxx$)—a single atom in the center of a region with 5 blank sites on either side—to the probability of ob-

serving a strip of 11 blank sites (*xxxxxxxxxxx*). If the system is nearly poisoned, such configurations are so rare that the statistical errors are large, although the formula (A4) permits the errors to be easily quantified. Fortunately, the behavior in the critical region near the phase transition is dominated by long-range interactions, and we can appeal to conventional equilibrium phase transitions to argue that errors in the values of the short-range couplings will not change the critical behavior near a second-order phase transition.

---

*Present and permanent address.

[1]J. H. Barry and M. Khatun, Phys. Rev. B **35**, 8601 (1987); J. H. Barry, M. Khatun, and T. Tanaka, Phys. Rev. B **37**, 5193 (1988).

[2]H. B. Callen, Phys. Lett. **4B**, 161 (1963).

[3]M. E. Fisher, Phys. Rev. **113**, 969 (1959); see Ref. 1 and references therein.

[4]R. H. Swendsen, Phys. Rev. Lett. **52**, 1165 (1984); Phys. Rev. B **30**, 3866 (1984).

[5]P. Meakin and D. J. Scalapino, J. Chem. Phys. **96**, 731 (1987).

[6]R. M. Ziff, E. Gulari, and Y. Barshad, Phys. Rev. Lett. **56**, 2553 (1986).

[7]C. Tang and P. Bak, Phys. Rev. Lett. **60**, 2346 (1988) and J. Stat. Phys. (to be published); P. Bak, C. Tang, and K. Wiesenfeld, Phys. Rev. Lett. **59**, 381 (1987) and Phys. Rev. A **38**, 364 (1988).

[8]M. E. Fisher, J. Stat. Phys. **34**, 688 (1984); F. W. Weigel, in *Phase Transitions and Critical Phenomena*, edited by C. Domb and J. Liebowitz (Academic, London, 1987), Vol. 7, p. 109ff.

[9]R. Dickman, Phys. Rev. A **34**, 4246 (1986).

[10]G. Parisi, R. Petronzio, and F. Rapuano, Phys. Lett. **128B**, 418 (1983).

[11]M. Grunze (private communication); B. Yu, D. A. Browne, and P. Kleban (unpublished).

[12]R. J. Glauber, J. Math. Phys. **4**, 294 (1963).

[13]M. Gelfand (private communication).

[14]L. van Hove, Physica **15**, 951 (1949); L. D. Landau and E. M. Lifshitz, *Statistical Physics* (Pergamon, London, 1958), Sec. 149.